Green Chemistry

PAPER

View Article Online
View Journal | View Issue

Aqueous-phase hydrodeoxygenation of highly oxygenated aromatics on platinum†

Cite this: *Green Chem.*, 2014, **16**, 675

Jin Yang,[a] C. Luke Williams,[a] Ashwin Ramasubramaniam*[b] and Paul J. Dauenhauer*[a]

Utilization of renewable sugars from biomass by a hybrid chemical process produces highly oxygenated aromatic compounds, such as phloroglucinol, which require catalytic reduction for desirable aromatic products. Aqueous phase hydrodeoxygenation of phloroglucinol on carbon-supported platinum produces resorcinol, phenol, cyclohexanol, cyclohexanone, and 1,3-cyclohexanediol by combinations of carbon–oxygen bond cleavage and carbon–carbon double bond hydrogenation. Carbon–carbon σ-bond cleavage was not observed. Hydrodeoxygenation was the primary reaction of phloroglucinol, leading to the production of resorcinol in the overall rate-limiting reaction, with an activation energy barrier of E_a = 117 kJ mol^{-1}. Subsequent reactions of resorcinol produced 1,3-cyclohexanediol and phenol with similar energy barriers, E_a = 46 and E_a = 54 kJ mol^{-1}, respectively. Further hydrogenation of phenol (E_a = 42 kJ mol^{-1}) occurs through the intermediate, cyclohexanone, which is further reduced (E_a = 14 kJ mol^{-1}) to the dominant product, cyclohexanol.

Received 12th June 2013,
Accepted 13th August 2013

DOI: 10.1039/c3gc41138a

www.rsc.org/greenchem

1 Introduction

Six-carbon sugars naturally present in biomass have great potential to be a major renewable source of aromatic chemicals in the 21st century.[1,2] Basic chemical feedstocks such as ethylene, propylene and benzene come from fossil fuels including petroleum and natural gas. However, lignocellulosic biomass exists at sufficiently high quantities in the United States to supply the entire domestic chemical industry,[3,4] thereby providing a long-term feedstock and sustainable alternative to fossil fuel resources.

The widespread availability of biomass combined with its diverse chemical structure allows for multiple routes to production of aromatic chemicals. One potential route proposes to utilize lignin as a source of six-carbon aromatic feedstocks (20 to 30 wt% of hardwood trees[5]). As a polymer of oxygenated aromatic monomers (phenylpropane units), lignin can be depolymerized to produce a mixture of oxygenated aromatic chemicals including phenols, benzenediols, guaiacols and syringols[6,7] by a variety of catalytic technologies.[8] Subsequent hydrodeoxygenation of lignin monomers can then selectively cleave oxygen-containing functional groups (including hydroxyl, methoxy, and ketone) to targeted chemical products.[9–11]

Biomass can also be utilized for aromatic chemicals utilizing feedstock sugars including glucose and hemicellulose-derived monomers such as xylose.[12] Sugars readily form aromatic furan structures enabled by acid catalysts including furfural and hydroxymethylfurfural.[13,14] It was recently demonstrated that Diels–Alder cycloaddition of ethylene with furans and subsequent dehydration produces a six-carbon aromatic ring.[15,16] This approach allows for the catalytic production of a variety of alkylated aromatic chemicals including *p*-xylene at high selectivity.[17]

An alternative route to aromatic chemicals from sugars utilizes a hybrid process, in which both enzymatic and inorganic catalysts are utilized to achieve optimum process viability. As shown in Scheme 1, the cellulose/starch monomer, glucose, is selectively converted to *myo*-inositol,[18] a "bridge molecule" between technology platforms, which can subsequently be

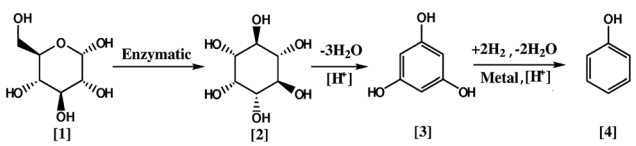

Scheme 1 Proposed process for hybrid production of aromatic products from glucose. Initial conversion of D-Glucose [1] to the "bridge molecule" *myo*-inositol [2] occurs through enzymatically driven cyclization to a six-carbon polyol ring. *Myo*-inositol can then be converted through dehydration to phloroglucinol [3], and catalytic hydrodeoxygenation forms phenol [4].

[a]*Department of Chemical Engineering, University of Massachusetts Amherst, Amherst, Massachusetts 01003, USA. E-mail: dauenhauer@ecs.umass.edu*
[b]*Department of Mechanical and Industrial Engineering, University of Massachusetts Amherst, Amherst, Massachusetts 01003, USA. E-mail: ashwin@engin.umass.edu*

†Electronic supplementary information (ESI) available. See DOI: 10.1039/c3gc41138a

dehydrated to oxygenated aromatic chemicals such as phloroglucinol (1,3,5-trihydroxy-benzene).[19] By combining the high selectivity of enzymes,[20] with the high turnover frequencies of thermochemical catalysts,[21] it is possible to develop entirely new processes for biorenewable chemicals. The potential of the process in Scheme 1 for producing valuable oxygenated aromatics, such as phenol or resorcinol from sugars, will depend on the catalytic capability for selectively reducing highly oxygenated chemicals like phloroglucinol.

The challenge of reducing biomass-derived molecules is broadly relevant due to the tendency of the photosynthetic process for producing oxygen-rich molecules.[22] Reduction of carbon by hydrogenation or hydrodeoxygenation (HDO)[23] of biomass-derived molecules, which can be up to 60 wt% oxygen,[24] is necessary to produce conventional chemicals as well as to reduce reactivity and viscosity[24–26] for storage and transportation. Transition metal catalysts such as Pt, Pd, and Ni have been widely studied for hydrogenation/HDO of biomass-derived molecules such as phenolics.[27–30] Additionally, NiMo, NiW and CoMo sulfides have been used for hydrodeoxygenation of biomass-derived bio-oils,[31–33] but the introduction of sulfur into the process is required to maintain catalytic activity. Noble metals supported on Si- and Al-based zeolites,[34] which provide Brønsted acidity,[35] have been widely studied. In these systems, it is reported that the overall reaction utilizes a combination of metal-catalyzed hydrogenation reactions (on metal surfaces) and acid-catalyzed dehydration reactions (with the support).[36]

In this work, metal catalysis for hydrogenation/HDO of oxygenated aromatics including phloroglucinol, resorcinol and phenol was investigated using an inert carbon support. Platinum was selected for fundamental study due to its previously described capability for hydrogenation of aromatic C=C and C=O bonds to produce cyclohexanol from aromatic compounds.[37–40] All experiments utilizing phloroglucinol, a low volatility chemical, were conducted in liquid water with the goal of providing experimental insight into the impact of aqueous solvent on a wide range of biomass-derived oxygenated chemical reactions for the advancement of green chemistry.

2. Experimental description

Experiments were conducted in a liquid phase reactor at high hydrogen gas pressure utilizing carbon-supported Pt catalysts.

2.1 Materials

5 wt% Pt/C catalysts were purchased from Sigma Aldrich (#205931). H_2 chemisorption using an Autosorb iQ_2 (Quantachrome AS IQC002) was used to determine the catalyst Pt surface area of 3.98 $m^2\ g^{-1}$. Carbon support material was also purchased from Sigma-Aldrich (#484164). Reactant chemicals including phloroglucinol (Alfa Aesar, #B25502), resorcinol (Sigma-Aldrich, #A13080) and Phenol (Alfa Aesar, #33213) were purchased at 98% purity or higher and used as received. All gases were purchased form Middlesex Gas Company and were of Ultrahigh Purity (UHP) or, in the case of air, grade 5.0.

2.2 Reactor

Reactions were carried out in a one liter, high-pressure, high-temperature Parr benchtop reactor (Model 4581 with a PARR 4842 temperature controller) using 5 wt% Platinum on carbon catalysts. Phloroglucinol (Alfa Aesar, anhydrate, 98%) was reacted with H_2 on Pt/C catalyst over a temperature range of 190–230 °C at a loading of 1.0 gram of catalyst to 500 ml of water (0.2 wt% phloroglucinol). Hydrogenation of resorcinol (Alfa Aesar, 99%) and phenol (Alfa Aesar, 99%) was also examined over a temperature range of 40–125 °C. Experimental trials were concluded when conversion exceeded 90%, and carbon balances for all reactions reached 85% or higher. The reaction vessel was purged with nitrogen and stirred at ~1000 rpm with a gas entrainment impeller while heating up to the reaction temperature. For all reactions at various temperatures, hydrogen gas was added to the reactor headspace up to 800 psi after the desired reaction temperature was achieved. Gas was continuously added during the experiment to maintain a constant operating pressure and solution concentration. Liquid samples were collected by pressure-driven flow through a filter to a sample tube; the liquid sample was cooled to room temperature and then collected in sample vials. The first sample was collected immediately after pressurization with H_2 as an initial data point. Samples were collected during the reaction until the conversion exceeded 90%. Later, 50 μl of 5 vol% 2-buten-1-ol (Alfa Aesar, *cis* + *trans* 96%) in water was added as an external standard to 1000 μl of reaction sample. Products were identified using a gas chromatograph (Agilent 7890A) equipped with a flame ionization detector (FID). Additional analysis of less volatile compounds was conducted using a high performance liquid chromatograph (UFLC LC-20AD), using a Waters Hi-Plex Na 10 μm column.

2.3 Gas–liquid mass transfer

The second Damköhler number was determined to evaluate the relative rates of reaction and gas-to-liquid mass transfer. A series of experiments for phenol hydrogenation at 125 °C were conducted to obtain the reaction constant k_{rxn} under the fastest reaction conditions. Independent H_2 mass transfer tests were performed by adding 500 ml water to the reactor and pressurizing to 800 psi H_2 without catalysts at room temperature; these conditions were purposely selected to characterize interphase H_2 transfer at the slowest possible conditions. Once the reactor achieved steady pressure, the gas entrainment impellor was turned to 1000 rpm and the vessel pressure was monitored with $1/15^{th}$ of a second resolution. The slope of the plot of the logarithm of the hydrogen pressure change *versus* time led to the measurement of mass transport rate, k_La (Fig. 1). The second Damköhler number, defined as the ratio k_{rxn}/k_la, was found to be 0.2, which indicates that the slowest rate of mass transfer of the H_2 to the liquid was faster than the rate of consumption in the hydrogenation of phenol, thereby eliminating H_2 interphase mass transfer limitations.

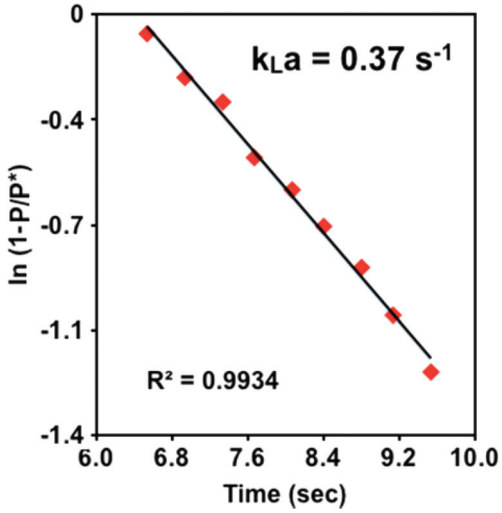

Fig. 1 Characterization of hydrogen gas–liquid mass transfer. H_2 pressure change upon the start of the gas dispersion impeller was used for calculation of the mass transfer coefficient (k_La). *P* is the hydrogen gas pressure change at time *t*, while *P** is the maximum hydrogen pressure at saturation.

3. Results and discussion

The complex nature of hydrogenation/hydrodeoxygenation of phloroglucinol leads to multiple reaction pathways and a set of associated activation energy barriers and effective rate constants. There exist several possible reactions of phloroglucinol including hydrogenation of C–C π bonds (aromatic ring), hydrodeoxygenation of C–OH groups, and C–C σ-bond cleavage. In order to evaluate the role of the carbon support on these reactions, blank tests were conducted using only the carbon support in water with phloroglucinol reactant. This reaction at 300 °C and 800 psi H_2 exhibited no detectable change in phloroglucinol concentration after 3 hours, which indicates that neither homogeneous reactions of phloroglucinol nor phloroglucinol-support reactions are significantly involved in the overall hydrogenation/HDO process. An additional experiment, utilizing Pt/C catalyst with an inert N_2 atmosphere (no H_2) was also conducted to demonstrate no significant homogeneous reaction of phloroglucinol. Thus, non-catalytic reactions of phloroglucinol are expected to be negligible in our experiments.

3.1 Hydrogenation of phloroglucinol

The main products observed from hydrogenation of phloroglucinol were resorcinol, 1,3-cyclohexanediol, and cyclohexanol, all of which retain the six-carbon ring structure. The concentrations of all chemical species are shown with respect to time in Fig. 2, where a significant variation in reaction rate is evident as reaction temperature changes (Fig. 2A–E). An increase in the reaction temperature by 40 °C (from 190 °C to 230 °C) increases the reaction rate by an order of magnitude. Additionally, the chemical 1,3,5-cyclohexanetriol was not detected in the products, indicating that direct hydrogenation

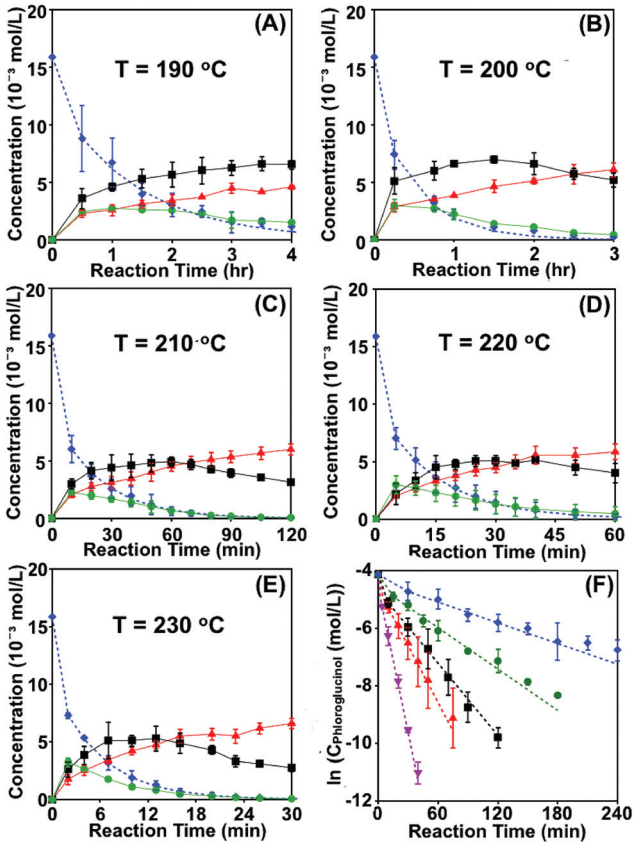

Fig. 2 Hydrogenation of Phloroglucinol. Reaction of phloroglucinol (◆) and hydrogen produces resorcinol (●), 1,3-cyclohexanediol (■), and cyclohexanol (▲) at (A) 190 °C, (B) 200 °C, (C) 210 °C, (D) 220 °C, (E) 230 °C. Panel (F) shows the logarithm of concentration of phloroglucinol *versus* time at different temperatures: 190 °C (◆), 200 °C (●), 210 °C (■), 220 °C (▲), and 230 °C (▼). Solid markers represent experimental data, while dashed lines are modeled concentrations using fitted kinetic parameters.

of C–C π-bonds of phloroglucinol does not likely occur. Furthermore, the concentration of resorcinol initially increases before decreasing, indicating that resorcinol is an intermediate of phloroglucinol hydrogenation and is subsequently consumed in additional hydrogenation steps (Section 3.2). Thus, we conclude that hydrodeoxygenation, rather than direct hydrogenation of the aromatic ring, is the first reaction in the process of phloroglucinol hydrogenation.

An additional experiment to examine 1,3-cyclohexanediol dehydration (followed by hydrogenation) to cyclohexanol (800 psi H_2) was performed, from which we found that no significant reaction was observed at temperatures below 200 °C (also evidenced in Fig. 2). At temperatures above 200 °C, hydrodeoxygenation of 1,3-cyclohexanediol to cyclohexanol becomes the dominant reaction (Fig. 2B–E), particularly when the concentration of phloroglucinol is very low.

3.2 Hydrogenation of resorcinol

As shown in Fig. 2, resorcinol concentrations (green line) exhibit a maximum throughout the HDO of phloroglucinol,

which indicates that resorcinol is an important intermediate requiring further examination. Initial experiments examined the hydrogenation of resorcinol at 200 °C and 800 psi H_2, but the reaction was observed to occur too fast for experimental characterization. Hence, additional experiments were conducted at a lower range of temperatures between 40–125 °C. All experiments were carried out until 90% resorcinol conversion was achieved and all carbon balances closed at 90% or greater. Hydrogenation of resorcinol produced primarily 1,3-cyclohexanediol and cyclohexanol, but small quantities (1.5 mol%) of phenol were detected at the beginning of the reaction (resorcinol conversion <3%). The concentration of resorcinol and all measured products are shown in Fig. 3.

The hydrogenation of resorcinol appears to produce 1,3-cyclohexanediol and cyclohexanol by parallel, competing pathways. Hydrodeoxygenation of 1,3-cyclohexanediol does not appear to produce cyclohexanol within the studied reaction temperature range, which indicates that another reaction intermediate must exist in the process of cyclohexanol production. A possible reaction intermediate is phenol, which is detected at low concentrations (<1.5 mol%) at early reaction times in Fig. 3. It is also observed in Fig. 3 that the product distribution shifts from favoring 1,3-cyclohexanediol (black line) to cyclohexanol (red line) as temperature increases. This result indicates that direct hydrogenation of the aromatic ring yields 1,3-cyclohexanediol at low temperature. However, at the high temperature of 125 °C shown in Fig. 3E, hydrogenation/dehydration of resorcinol to phenol, followed by hydrogenation to cyclohexanol, overwhelms the direct hydrogenation of the aromatic ring.

3.3 Hydrogenation of phenol

As shown in Fig. 3, hydrogenating resorcinol mainly yields 1,3-cyclohexanediol and cyclohexanol without dehydration. The intermediate, phenol, which can be detected in the very initial stages, was therefore additionally investigated for the range of 40–125 °C at 800 psi H_2. All experiments were carried out until 95% phenol conversion was achieved, and all carbon balances closed at 95% or greater. The concentration of phenol and all detected intermediates and products *versus* time are shown in Fig. 4.

Cyclohexanone concentrations (orange line in Fig. 4A–E) exhibit a maximum throughout the hydrogenation reactions,

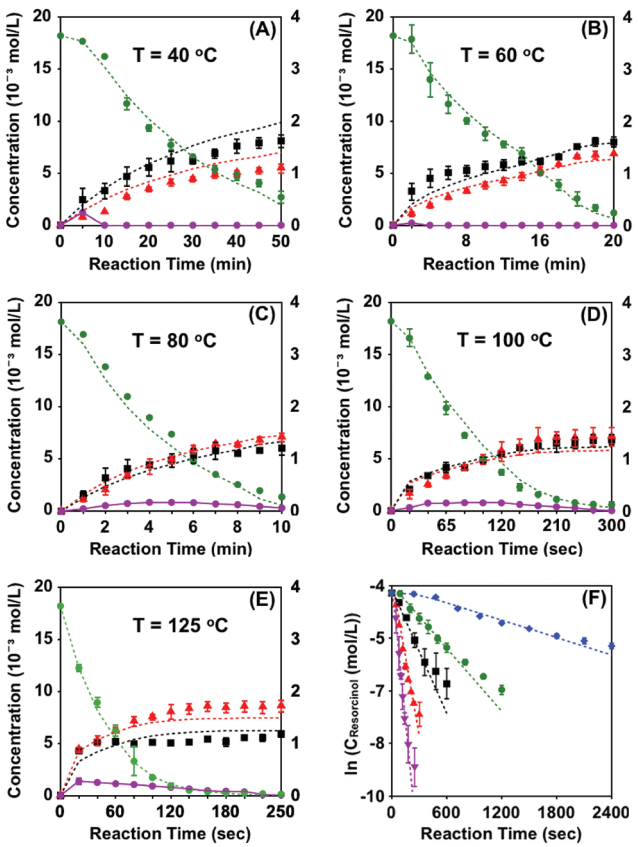

Fig. 3 Hydrogenation of Resorcinol. The reaction of resorcinol (●) and hydrogen produces 1,3-cyclohexanediol (■), cyclohexanol (▲) and phenol (●, using right y axis) at (A) 40 °C, (B) 60 °C, (C) 80 °C, (D) 100 °C, (E) 125 °C. Panel (F) shows the logarithm of concentration of resorcinol *versus* time at 40 °C (◆), 60 °C (●), 80 °C (■), 100 °C (▲), and 125 °C (▼). Solid markers represent experimental data, while dashed lines are model concentrations using fitted kinetic parameters.

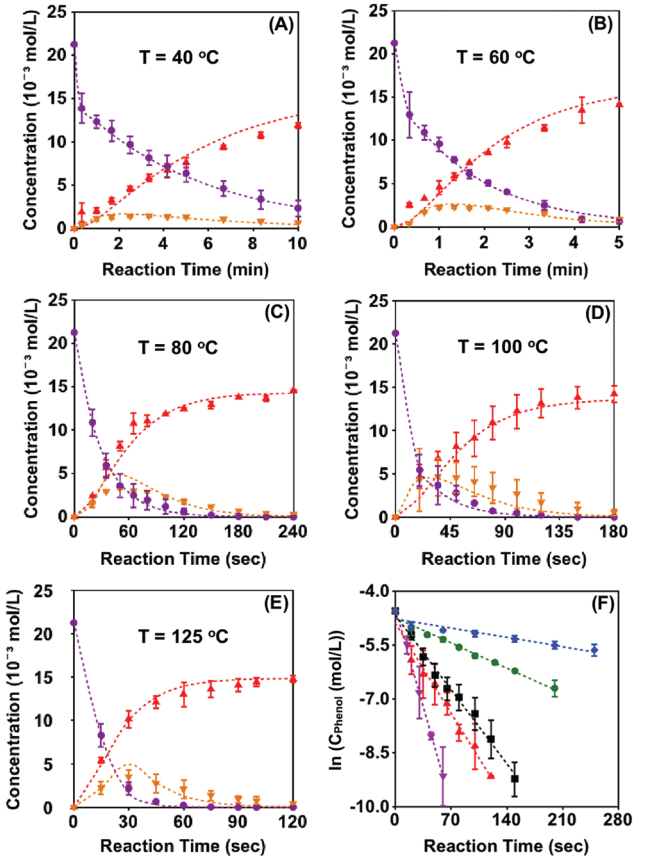

Fig. 4 Hydrogenation of Phenol. The reaction of phenol (●) and hydrogen produces cyclohexanone (▼), and cyclohexanol (▲) at (A) 40 °C, (B) 60 °C, (C) 80 °C, (D) 100 °C, (E) 125 °C. Panel (F) shows the logarithm of phenol concentration *versus* time at 40 °C (◆), 60 °C (●), 80 °C (■), 100 °C (▲), and 125 °C (▼). Solid markers represent experimental data, while dashed lines are modeled concentrations using fitted kinetic parameters.

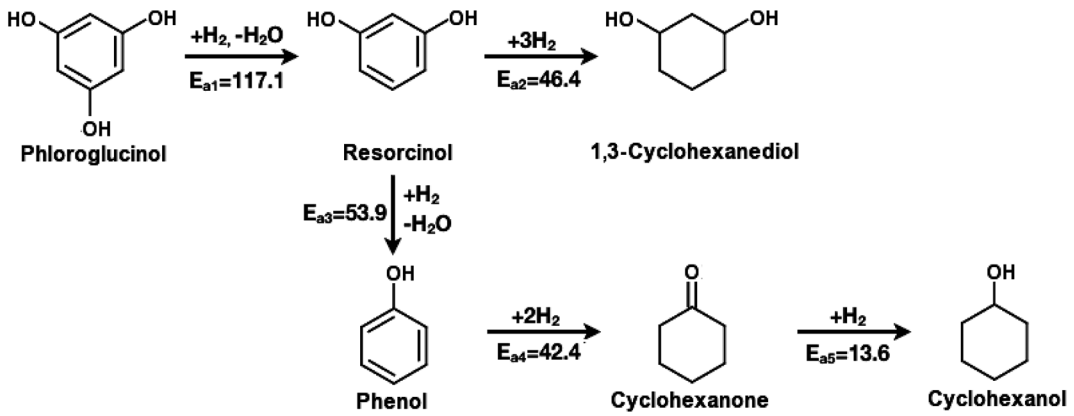

Scheme 2 Reaction scheme for hydrogenation of phloroglucinol. Numbers below arrows represent the experimentally determined activation energy (in kJ mol^{-1}) associated with each reaction.

Table 1 Effective reaction rate constants and activation barrier for hydrogenation of phloroglucinol ($k_{eff,1}$) at five reaction temperatures

T (°C)	190	200	210	220	230	E_{a1} (kJ mol^{-1})
$k_{eff,1}$ (10^3 s^{-1})	0.2 ± 0.03	0.5 ± 0.01	0.8 ± 0.2	1.1 ± 0.3	2.8 ± 0.6	117.1 ± 12.9

which indicates that cyclohexanone is an intermediate that undergoes further hydrogenation to cyclohexanol. Also, based on satisfactorily high carbon balance closure (>95%), it can be determined that undetected species exist at negligible concentration and there is negligible C–C σ-bond breaking. Our experiments agree well with previous studies; hydrogenation of phenol with Pt catalyst results in the formation of cyclohexanol as a final product *via* cyclohexanone as an intermediate.[41]

3.4 Kinetic model

A kinetic description of the reaction network for the hydrogenation of phloroglucinol, described by experimental data of Fig. 2–4, was developed by fitting global rate expressions to the considered reaction pathways of Scheme 2. Kinetic expressions were utilized within a batch reactor model with fixed volume of liquid water. Based on the H_2 mass transfer rates discussed in section 2.3, it was assumed that the concentration of H_2 in the water was constant. Organic reactants were described using first order kinetics based on kinetic fitting of the data (Fig. 2F, 3F and 4F) with activation energies obtained from Arrhenius expressions of kinetic rate coefficients. It was assumed that adsorption/desorption was at equilibrium.

Hydrogenation of phloroglucinol data (Fig. 2) was fit to a second-order rate expression, which was simplified to a first-order expression utilizing an effective rate coefficient by assuming constant concentration of H_2 in water (at saturation),

$$\frac{dC_{\text{phloroglucinol}}}{dt} = -k_1 C_{H_2} C_{\text{phloroglucinol}} = -k_{\text{eff},1} C_{\text{phloroglucinol}}. \quad (1)$$

Non-linear least squared regression was applied to the raw data of Fig. 2 to obtain the reaction rate coefficients of Table 1. The resulting concentration profiles predicted by the determined rate parameters are plotted as dashed lines in Fig. 2, which are observed to agree well with the experimental data. An Arrhenius plot in Fig. 5A based on the measured rate coefficients exhibited linear behavior over the considered temperature range, indicating a single rate limitation which was experimentally determined (based on the observed products) to be the hydrodeoxygenation of phloroglucinol with an activation energy barrier of 117.1 ± 12.9 kJ mol^{-1}.

Hydrogenation/dehydration of resorcinol was kinetically described using two parallel first-order reactions describing (i) hydrogenation to 1,3-cyclohexanediol, and (ii) hydrogenation/dehydration to phenol,

$$\frac{dC_{1,3\text{-cyclohexanediol}}}{dt} = k_2 C_{H_2} C_{1,3\text{-cyclohexanediol}} = k_{\text{eff},2} C_{1,3\text{-cyclohexanediol}}, \quad (2)$$

$$\frac{dC_{\text{phenol}}}{dt} = k_3 C_{H_2} C_{\text{phenol}} = k_{\text{eff},3} C_{\text{phenol}}, \quad (3)$$

$$\frac{dC_{\text{resorcinol}}}{dt} = -(k_2 + k_3) C_{H_2} C_{\text{resorcinol}} = k_{\text{eff},2} C_{1,3\text{-cyclohexanediol}} + k_{\text{eff},3} C_{\text{phenol}}, \quad (4)$$

where k_2 and k_3 are the respective rate coefficients for the forward reactions. The kinetic descriptions of eqn (2)–(4) were fit to the experimental data of Fig. 3 by the following method. The overall rate of resorcinol consumption was fit to the resorcinol concentration data at each temperature to determine the combined effective rate constants ($k_{eff,2}$ + $k_{eff,3}$). Subsequently, the rate coefficient for generation of 1,3-cyclohexanediol ($k_{eff,2}$) was obtained by fitting eqn (2) to the concentration of 1,3-cyclohexanediol from Fig. 3 at each temperature.

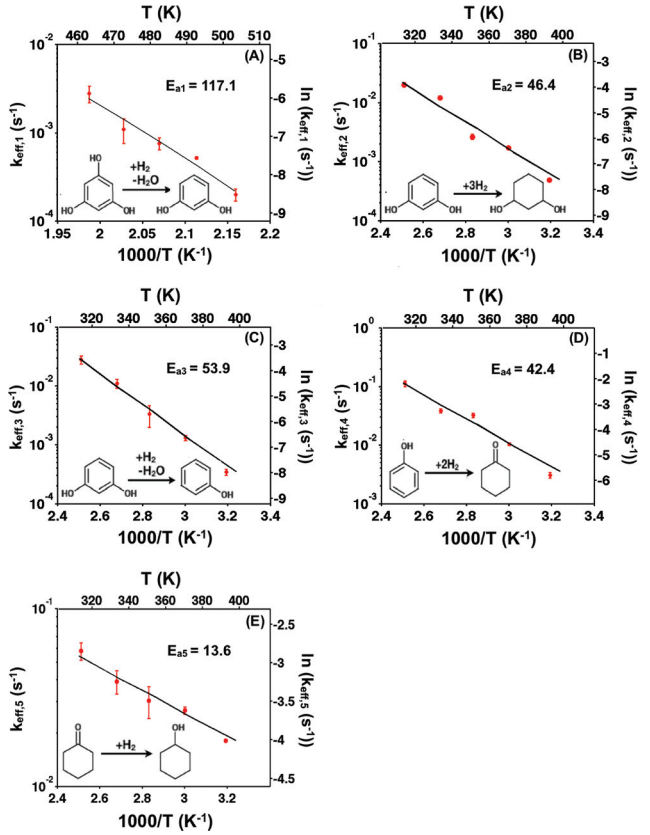

Fig. 5 Activation energies of major reaction pathways of phloroglucinol hydrogenation. Arrhenius plots of: (A) HDO of phloroglucinol, (B) hydrogenation of resorcinol to 1,3-cyclohexanediol, (C) hydrogenation/dehydration of resorcinol to phenol, (D) hydrogenation of phenol, and (E) hydrogenation of cyclohexanone. (Units: kJ mol^{-1}).

The concentration of phenol was obtained from a mass balance of resorcinol and 1,3-cyclohexanediol, and the rate coefficient for phenol generation ($k_{eff,3}$) was fit to the phenol concentration using eqn (3). The estimated concentrations of major species are shown by dashed lines in Fig. 2, which shows excellent agreement with the experimental data.

Hydrogenation of phenol was described using two, sequential first-order reactions describing (i) hydrogenation to cyclohexanone, and (ii) hydrogenation to cyclohexanol, as

$$\frac{dC_{phenol}}{dt} = -k_4 C_{H_2} C_{phenol} = -k_{eff,4} C_{phenol}, \quad (5)$$

$$\frac{dC_{cyclohexanone}}{dt} = k_4 C_{H_2} C_{phenol} - k_5 C_{H_2} C_{cyclohexanone} = k_{eff,4} C_{phenol} - k_{eff,5} C_{cyclohexanone} \quad (6)$$

where k_4 and k_5 are the respective rate coefficients for the forward reactions. The consumption rate of phenol was fit to phenol concentration data at each temperature to obtain the effective rate constant, $k_{eff,4}$. Once $k_{eff,4}$ was obtained, the hydrogenation rate of cyclohexanone, $k_{eff,5}$, was determined by fitting eqn (6) using both phenol and cyclohexanone concentration data. Estimated concentrations of major species are shown in dashed lines of Fig. 4, which shows good agreement with experimental data. The complete set of reaction rate coefficients are listed in Table 2.

Activation barriers, determined from the experimentally-fit rate coefficients, are consistent with the proposed reaction pathways of Scheme 2. Arrhenius plots of the reaction rate coefficients are depicted in Fig. 5 and reveal the kinetic energy barriers associated with each pathway. The barrier for HDO reaction of phloroglucinol to produce resorcinol from phloroglucinol was measured to be 117.1 ± 12.9 kJ mol^{-1}. This barrier is considerably higher than other barriers in these experiments and confirms that the removal of a single hydroxyl group from phloroglucinol (*i.e.*, HDO) is the slowest reaction in the overall process.

Competing reaction pathways of resorcinol exhibit significantly lower barriers than HDO of phloroglucinol. The Arrhenius plot for hydrogenation to 1,3-cyclohexanediol (Fig. 5B) indicates a barrier of 46.4 ± 4.7 kJ mol^{-1}, while the Arrhenius plot for hydrogenation/dehydration to phenol (Fig. 5C) exhibits a barrier of 53.9 ± 1.7 kJ mol^{-1}. Similarly, Arrhenius plots indicate a reaction barrier of 42.4 ± 4.2 kJ mol^{-1} to hydrogenate phenol (Fig. 5D), while the barrier of the sequential hydrogenation of cyclohexanone (Fig. 5E) is 13.6 ± 1.2 kJ mol^{-1}.

From the above results, it is clear that the barriers to hydrogenate the aromatic ring are similar; for example, hydrogenating resorcinol to 1,3-cyclohexanediol requires 46.4 kJ mol^{-1} while hydrogenating phenol to cyclohexanone requires 42.4 kJ mol^{-1}. This is not surprising as these reactions involve breaking C–C π-bonds. However, the barrier for removal of one hydroxyl group from phloroglucinol is about twice as large as that for removal of a hydroxyl group from resorcinol, which indicates substantially different reaction mechanisms.

We propose that an H atom on the Pt surface cannot directly hydrogenate the phloroglucinol aromatic ring, due to the significant steric hindrance posed by the three OH groups. In previous work, we have shown that phloroglucinol forms an

Table 2 Effective reaction rate constants, k, and activation barriers, E_a, for hydrogenation of resorcinol ($k_{eff,2}$ and $k_{eff,3}$), phenol ($k_{eff,4}$), and cyclohexanone ($k_{eff,5}$) at five reaction temperatures

T (°C)	40	60	80	100	125	E_a (kJ mol^{-1})
$k_{eff,2}$ (10^3 s^{-1})	0.48 ± 0.02	1.7 ± 0.1	2.6 ± 0.3	12.0 ± 1.0	20.0 ± 1.7	46.4 ± 4.7
$k_{eff,3}$ (10^3 s^{-1})	0.34 ± 0.04	1.3 ± 0.1	3.3 ± 1.3	11.0 ± 1.8	28.0 ± 4.3	53.9 ± 1.7
$k_{eff,4}$ (10^3 s^{-1})	3.0 ± 0.3	10.2 ± 0.4	33.4 ± 2.9	35.8 ± 3.3	89.1 ± 1.9	42.4 ± 4.2
$k_{eff,5}$ (10^3 s^{-1})	17.8 ± 0.3	26.6 ± 1.3	30.3 ± 6.3	39.3 ± 5.8	58.3 ± 6.5	13.6 ± 1.2

H-bond network with its surrounding water molecules. Hence, aromatic carbons in phloroglucinol are blocked from direct hydrogenation. Instead, the hydrogen atom on the surface tends to bond to the oxygen atom of the hydroxyl group and breaks the C–O bond,[42] which is already weakened upon chemisorption on Pt, to form a water molecule. In contrast, with the absence of one hydroxyl group in resorcinol, the aromatic ring can be directly hydrogenated; the hydrogenation step is then followed by dehydration to form phenol. The barrier for the hydrogenation/dehydration of resorcinol (53.9 kJ mol^{-1}) is only slight greater than that of direct hydrogenation of the ring (46.4 kJ mol^{-1} or 42.4 kJ mol^{-1}), which supports the hypothesis that hydrogenation/dehydration of resorcinol reaction is limited by hydrogenation of the aromatic ring. Literature provides a wide range for the barrier for HDO reaction of small molecules, ranging between 50 kJ mol^{-1} (experimental) and 150 kJ mol^{-1} (simulation) in gas phase reaction,[43,44] and bond dissociation energy for a Ph–OH bond has been shown to be much higher than that for a Ph–H bond.[45] This agrees well with our experimental observation; the limiting reaction for HDO of phloroglucinol, which we propose to be C–O bond breaking, is much slower than that of hydrogenation/dehydration of resorcinol, which is thought to be limited by hydrogenation of the C–C π-bond.

4. Conclusions

Hydrogenation reactions of highly oxygenated species including phloroglucinol, resorcinol and phenol have been examined to understand the competing reaction pathways of C–O, C–C and C=C cleavage on carbon-supported Platinum. For the considered reaction conditions, hydrogenation of these biomass intermediates maintains the six-carbon ring structure. Direct hydrogenation of the carbon ring of phloroglucinol does not appear to occur, which is attributed to steric hindrance of three hydroxyl groups and surrounding water molecules. Hydrodeoxygenation of phloroglucinol by direct C–OH cleavage removes the first hydroxyl group to produce resorcinol in the overall rate-limiting reaction with activation energy barrier of 117.1 kJ mol^{-1}. Subsequent competing reaction pathways of resorcinol occur include hydrogenation to 1,3-cyclohexanediol (E_a = 46 kJ mol^{-1}) and hydrogenation/dehydration to phenol (E_a = 54 kJ mol^{-1}). For both reactions, breaking of ring aromaticity is the limiting step, as evidenced by similar reaction energy barriers. Further hydrogenation of phenol (E_a = 42 kJ mol^{-1}) produces cyclohexanone, which is further hydrogenated (E_a = 14 kJ mol^{-1}) to cyclohexanol.

Acknowledgements

Jin Yang and Paul Dauenhauer acknowledge support from the 3M Corporation Nontenured Faculty Award. Ashwin Ramasubramaniam acknowledges startup support from the University of Massachusetts Amherst.

References

1 K. Sanderson, *Nature*, 2006, **444**, 673–676.
2 A. J. Ragauskas, *et al.*, *Science*, 2006, **311**, 484–489.
3 R. D. Perlack, L. L. Wright, A. F. Turhollow, R. L. Graham, B. J. Stokes and D. C. Erbach, *Biomass as a Feedstock for a Bioenergy and Bioproducts Industry: The Technical Feasibility of a Billion-Ton Annual Supply*, Oak Ridge National Laboratory, Oak Ridge, TN, 2005.
4 R. D. Perlack and B. J. Stokes, *U.S. Billion-Ton Update: Biomass Supply for a Bioenergy and Bioproducts Industry*, Oak Ridge National Laboratory, Oak Ridge, TN, 2011.
5 M. E. Himmel, K. Tatsumoto, K. K. Oh, K. Grohmann, D. K. Johnson and H. L. Chum, *ACS Symp. Ser.*, 1988, **397**, 82–89.
6 M. Garcia-Perez, A. Chaala, H. Pakdel, D. Kretschmer and C. Roy, *Biomass Bioenergy*, 2007, **31**, 222–242.
7 J. P. Diebold, in *Fast pyrolysis of biomass: A handbook*, ed. A. V. Bridgwater, *et al.*, CPL Press, Newbury, UK, 2002.
8 V. M. Roberts, V. Stein, T. Reiner, A. Lemonidou, X. Li and J. A. Lercher, *Chem. Eng. J.*, 2011, **17**, 5939–5948.
9 C. Zhao and J. A. Lercher, *ChemCatChem*, 2012, **4**(1), 64–68.
10 R. C. Runnebaums, R. J. Lobo-Lapidus, T. Nimmanwudipong, D. E. Block and B. C. Gates, *Energy Fuels*, 2011, **25**, 4776–4785.
11 P. T. M. Do, A. J. Foster, J. Chen and R. F. Lobo, *Green Chem.*, 2012, **14**, 1388–1397.
12 D. G. Vlachos, J. G. Chen, R. J. Gorte, G. W. Huber and M. Tsapatsis, *Catal. Lett.*, 2010, **140**(3–4), 77–84.
13 V. Choudary, A. B. Pinar, S. I. Sandler, D. G. Vlachos and R. F. Lobo, *ACS Catal.*, 2011, **1**(12), 1724–1728.
14 V. Choudary, S. H. Mushrif, C. Ho, A. Anderko, V. Nikolakis, N. S. Marinkovic, A. I. Frenkel, S. I. Sandler and D. G. Vlachos, *J. Am. Chem. Soc.*, 2013, **135**(10), 3997–4006.
15 C. Chang, S. K. Green, C. L. Williams, P. J. Dauenhauer and W. Fan, *Green Chem.*, 2013, DOI: 10.1039/c3gc40740c.
16 N. Nikbin, P. T. Do, S. Caratzoulas, R. F. Lobo, P. J. Dauenhauer and D. G. Vlachos, *J. Catal.*, 2013, **297**, 35–43.
17 L. C. Williams, C. Chang, P. Do, N. Nikbin, S. Caratzoulas, D. G. Vlachos, R. F. Lobo, W. Fan and P. J. Dauenhauer, *ACS Catal.*, 2012, **2**(6), 935–939.
18 K. Sanderson, *Nature*, 2006, **444**, 673–676.
19 L. Rocha, A. Marston, O. Potterat, M. A. C. Kaplan and K. Hostettmann, *Phytochemistry*, 1996, **42**(1), 185–188.
20 S. Atssumi, T. Hanai and J. C. Liao, *Nature*, 2008, **451**, 86–89.
21 L. D. Schmidt and P. J. Dauenhauer, *Nature*, 2007, 447.
22 P. H. Raven, R. F. Evert and S. E. Eichhorn, *Biology of plants*, W.H. Freeman and Company Publishers, New York, 2005.
23 E. Furimsky, *Appl. Catal., A*, 2000, **199**, 147–190.
24 T. P. Vispute, H. Y. Zhang, A. Sanna, R. Xiao and G. W. Huber, *Science*, 2010, **330**, 1222.

25 A. Oasmaa and S. Czernik, *Energy Fuels*, 1999, **13**, 914–921.
26 M. M. Wright, D. E. Daugaard, J. A. Satrio and R. C. Brown, *Fuel*, 2010, **89**, S2–S10.
27 S. G. Shore, E. Ding, C. Park and M. A. Keane, *Catal. Commun.*, 2002, **3**, 77–84.
28 H. Liu, T. Jiang, B. Han, S. Liang and Y. Zhou, *Science*, 2009, **326**, 1250–1252.
29 C. Zhao, Y. Kou, A. A. Lemonidou, X. Li and J. A. Lercher, *Chem. Commun.*, 2010, **46**, 412–414.
30 E. Shin and M. A. Keane, *Ind. Eng. Chem. Res.*, 2000, **39**, 883–892.
31 Y. Romero, F. Richard and S. Brunet, *Appl. Catal., B*, 2010, **98**, 213–223.
32 M. Ferrari, R. Maggi, B. Delmon and P. Grange, *J. Catal.*, 2001, **198**(1), 47–55.
33 F. E. Massoth, P. Politzer, M. C. Concha, J. S. Murray, J. Jakowski and J. Simons, *J. Phys. Chem. B*, 2006, **110**, 14283–14291.
34 X. Zhu, L. L. Lobban, R. G. Mallinson and D. E. Resasco, *J. Catal.*, 2011, **281**, 21–29.
35 F. Yaripour, F. Baghaei, I. Schmidt and J. Perregaard, *Catal. Commun.*, 2005, **6**(2), 147–152.
36 A. J. Foster, P. T. M. Do and R. F. Lobo, *Top. Catal.*, 2012, **58**, 118–128.
37 M. Englisch, *J. Catal.*, 1997, **166**(1), 25–35.
38 H. Takagi, T. Isoda, K. Kusakabe and S. Morooka, *Energy Fuels*, 1999, **13**(6), 1191–1196.
39 K. Amouzegar and O. J. Savadogo, *Appl. Electrochem.*, 1997, **27**(5), 539–542.
40 A. Martel, B. Mahdavi, L. Jean, B. Louis and H. Menard, *Can. J. Chem.*, 1997, **75**(12), 1862–1867.
41 D. Hong, S. J. Miller, P. K. Agrawal and C. W. Jones, *Chem. Commun.*, 2010, **46**, 1038–1040.
42 J. Yang, P. J. Dauenhauer and A. Ramasubramaniam, *J. Comput. Chem.*, 2012, **34**(1), 60–66.
43 M. A. Alotaibi, E. F. Kozhevnikova and I. V. Kozhevnikov, *Chem. Commun.*, 2012, **48**, 7194–7196.
44 R. Alcala, M. Mavrikakis and J. A. Dumesic, *J. Catal.*, 2003, **218**, 178–190.
45 R. T. Sanderson, *Chemical Bonds and Bond Energy*, Academic Press, 1976.

